

High Time Resolution Photon Counting 3D Imaging Sensors

Oswald H. W. Siegmund, Camden D. Ertley, John V. Vallerga
Space Sciences Laboratory, U.C. Berkeley

ABSTRACT

Novel sealed tube microchannel plate (MCP) detectors using next generation cross strip (XS) anode readouts and high performance electronics have been developed to provide photon counting imaging sensors for Astronomy and high time resolution 3D remote sensing. 18 mm aperture sealed tubes with MCPs and high efficiency Super-GenII or GaAs photocathodes have been implemented to access the visible/NIR regimes for ground based research, astronomical and space sensing applications. The cross strip anode readouts in combination with PXS-II high speed event processing electronics can process high single photon counting event rates at >5 MHz (~ 80 ns dead-time per event), and time stamp events to better than 25 ps. Furthermore, we are developing a high speed ASIC version of the electronics for low power/low mass spaceflight applications. For a GaAs tube the peak quantum efficiency has degraded from $\sim 30\%$ (at 560 - 850 nm) to $\sim 25\%$ over 4 years, but for Super-GenII tubes the peak quantum efficiency of $\sim 17\%$ (peak at 550 nm) has remained unchanged for over 7 years. The Super-GenII tubes have a uniform spatial resolution of <30 μm FWHM ($\sim 1 \times 10^6$ gain) and single event timing resolution of ~ 100 ps (FWHM). The relatively low MCP gain photon counting operation also permits longer overall sensor lifetimes and high local counting rates. Using the high timing resolution, we have demonstrated 3D object imaging with laser pulse (630 nm 45 ps jitter Pilsas laser) reflections in single photon counting mode with spatial and depth sensitivity of the order of a few millimeters. A 50 mm Planacon sealed tube was also constructed, using atomic layer deposited microchannel plates which potentially offer better overall sealed tube lifetime, quantum efficiency and gain stability. This tube achieves standard alkali quantum efficiency levels, is stable, and has been coupled to the PXS-II electronics and used to detect and image fast laser pulse signals.

Keywords: Microchannel plate, GaAs, photon counting, imaging, timing

1. INTRODUCTION

We have utilized cross strip (XS) anodes in sealed tube microchannel plate detectors to provide high spatial and time resolution photon counting devices in the visible/NIR regime. The cross strip scheme senses microchannel plate charge signals on two orthogonal layers of strips and employs charge division and centroiding of the charge distribution to encode event X-Y positions. A variety of similar microchannel plate (MCP) photon counting, event timing, imaging detectors have found extensive use in astronomical [1-6], remote sensing [7], and biological imaging [8, 9] applications. Sealed tube configurations (Fig. 1) with proximity focus GaAs photocathodes [10] and with Super-GenII [11] photocathodes have been built. The XS sealed tube detector scheme (Fig. 1) has a photocathode that is deposited on the inside of the input window which converts light to photoelectrons. Photoelectrons cross a proximity gap and are detected and amplified by a pair of MCPs. These tubes use a pair of back to back 6 μm pore MCPs with 13° bias and achieve gains up to $\sim 2 \times 10^6$. The XS readout anode has two orthogonal sets of conductive strips covering a 22 mm area, with an active area of 18 mm (Fig. 3) defined by the photocathode size. The GaAs photocathodes provide quantum efficiency of $\sim 30\%$ in the 550 nm to 850 nm region, while the Super-GenII achieves $\sim 17\%$ in the 450 nm to 850 nm regime. Parallel Cross Strip (PXS-II) electronics encodes photon event positions and times by amplifying the charge signals on the strips, digitizing the values and calculating the charge spot centroid in both X and Y. Timing is provided coarsely by a clock stamp (~ 20 ns) and fine timing is provided by a separate amplifier and time to digital converter on the MCP output connector. Background rates are dominated by the thermionic noise of the photocathodes, which can be high for the GaAs photocathodes at room temperature (>200 kHz), however modest cooling to $\sim 0^\circ\text{C}$ results in significant reduction (~ 10) of the single photoelectron noise. We have also used MCPs [12] made by atomic layer depositions (ALD) on borosilicate micro-capillary arrays in a sealed tube Planacon device. ALD MCPs have similar characteristics to conventional microchannel plates [12], but ALD MCPs have low outgassing and minimal gain decreases over at least 7 C cm^{-2} of charge extraction [13] after tube processing. Planacon was implemented with the PXS-II electronics to demonstrate imaging and assessed for its overall stability.

2. CROSS STRIP SEALED TUBE DETECTORS

2.1 Sealed Tube Microchannel Plate Detector Design

The window of the sealed tube detectors is a standard borosilicate glass with a drop face to establish a small (<200 μm) MCP gap, and the bias is adjusted to optimize the transit time spread and event timing performance. Two 6 μm

pore 80:1 l/d MCPs with 13 degree bias provide sufficient electron gain ($\sim 10^6$) for high resolution imaging and timing using the cross strip anode. A 22 mm XS anode design that is compatible with ultra high vacuum devices was made using multi-layer metal and ceramic deposited onto an alumina substrate (Fig. 2) and then high temperature fired. The strips for both axes have ~ 0.6 mm pitch period and are configured to intercept $\sim 50\%$ of the charge on the strips of each axis. The individual strip signals on the inside of the vacuum in the detector are brought to the back of the anode using hermetically sealed vias through the alumina substrate. On the outer surface of the anode (Fig. 5) the strip signals are connected to a standard multi-pin connector, which then uses shielded ribbon cables to connect with the amplifier electronics (Fig. 9). Inside the tube the XS anode is positioned ~ 2.5 mm behind the MCP pair. To obtain optimal event position centroiding [11] the MCP-anode gap voltage is adjusted so that charge is collected on several neighboring fingers (Fig. 1).

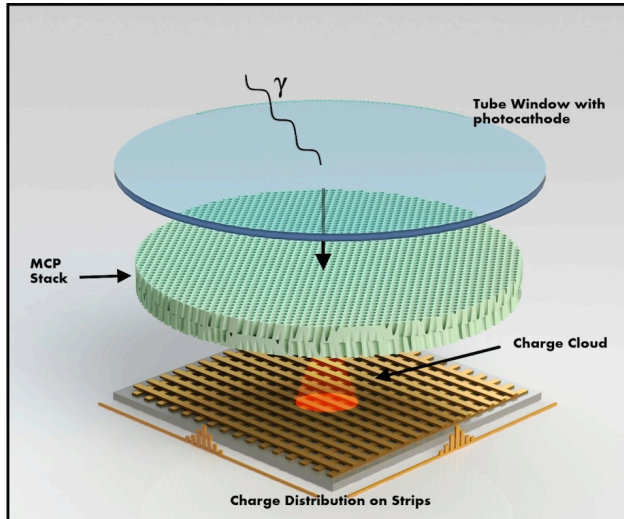


Fig. 1. Cross strip anode sensor scheme. Photons enter through a window inside of which is deposited a photocathode. Emitted photoelectrons are detected by the proximity focused MCPs and multiplied. This charge cloud is collected at the cross strip anode.

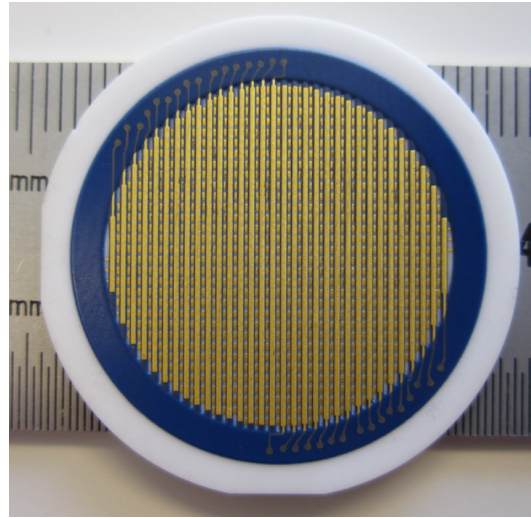


Fig. 2. A cross strip anode with a 22 mm area. This has upper and lower fingers (32 + 32) which collect the charge from the MCPs that falls on several adjacent strips for each event.

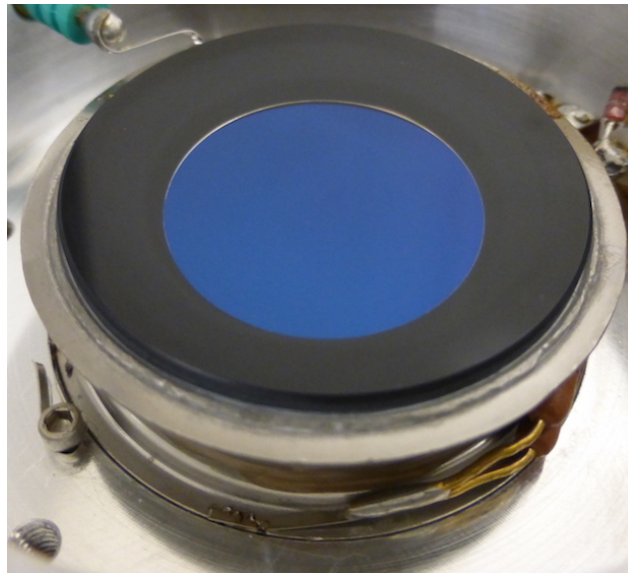


Fig. 3. A cross strip anode sealed tube sensor with a 22 mm readout anode, a pair of 6 μm pore 80:1 l/d MCPs and a GaAs photocathode,



Fig. 4. A cross strip anode sealed tube sensor with a 22 mm readout anode, a pair of 6 μm pore 80:1 l/d MCPs and a Super-GenII photocathode.

2.2 Sealed Tube Cross Strip Anode Microchannel Plate and Photocathode Performance

Sealed tubes with GaAs and Super-GenII photocathodes (Figs. 3, 4) were fabricated by Photonis-NL using 22 mm format XS anodes (Fig. 2). The distinctive color of the photocathodes are indicative of the response of these tubes, which ranges from ~400 nm to 900 nm. All of our tests were accomplished with the sealed tubes in a housing coupled to a preamplifier board (Fig. 6). The peak efficiency values are ~17% for Super-GenII tubes (at 550 nm) and ~30% for GaAs tubes. The room temperature dark rate for the GaAs sealed tubes is ~240 kHz and about 40 kHz for the Super-GenII tubes. However, with cooling the background rates drop to ~36 kHz at 8°C for GaAs photocathodes and <1500 Hz for Super-GenII photocathodes. The quantum efficiency of several of the sealed tubes was re-measured over a period of time (Figs. 7, 8). The two Super-GenII photocathode tubes show no significant change in quantum efficiency performance over seven years of intermittent use. We also have access to one of the three GaAs photocathode sealed tubes originally made. As shown in Fig. 8 there has been about a 20% loss in QE of a period of 4 years. The pairs of 6 μm pore 80:1 l/d, 13° bias MCPs used in these tubes reach gains of up to $\sim 2 \times 10^6$ at applied potential of ~1100 V per MCP. Pulse amplitude distributions for single photon events [14] is quite good (<100% FWHM) even at the low gain (1×10^6) which we employ with the XS readout. The low gain is a key factor in achieving high local event rate performance (>20 kHz, [11]) and long overall device lifetimes.

2.3 Position Encoding Electronics

In the PXS-II electronics scheme each strip on the anode (e.g. 32 X and 32 Y) is connected directly to a preamp input of a 32-channel ASIC, the "Preshape32", developed at Rutherford Appleton Laboratory (RAL) for the RD-20 collaboration [15]. The output of the amps are shaped unipolar pulses of ~40 ns rise time, ~400 ns fall time and a conversion gain of 0.72 mV / 1000 e⁻, with a noise floor of ~500+50/pF*C_{load} electrons. These 64 parallel outputs (32 x 2 axes) are amplified again (ADA4851-4) before being continuously digitized by 64 discrete 12-bit analog to digital converters (ADCs, Analog Devices ADS5271) operating at 50 mega-samples per second. These digital samples are fed into an FPGA (Xilinx Virtex6) using an LVDS serial stream of 600 MHz bit rate per ADC. In the FPGA pulse samples are digitally filtered to extract pulse peak information which are then passed to a circuit that uses the affected channels to determine the event centroid for both X and Y axes. This centroid position is combined with the digital timing signal determined by a coarse clock counter (20 ns) and a fine time (<20 ps) derived from a separate time to digital converter [16]. The events are buffered to await transfer to a downstream computer as an event list of X, Y and T (and pulse height) with the appropriate number of bits for the application.

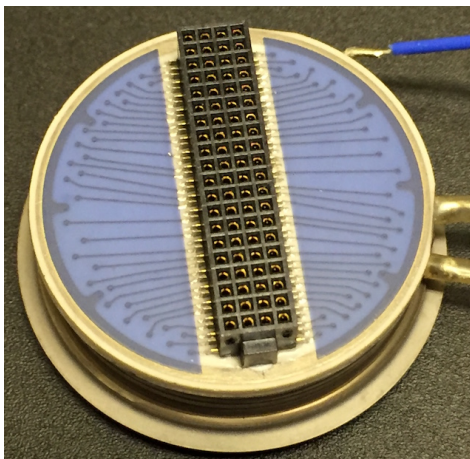


Fig. 5. 22 mm cross strip anode on a sealed tube with the signal connector mounted to the back face of the anode. Fan-in traces connect to through vias that are attached to the inside strips.

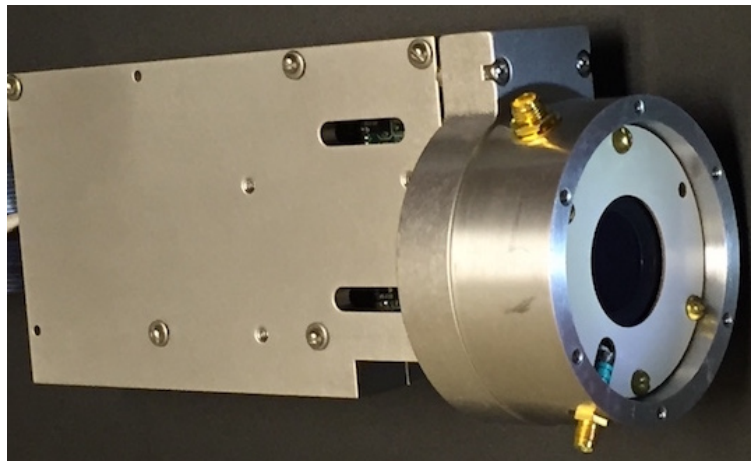


Fig. 6. A cross strip anode sensor with a 22 mm anode in a sealed tube mounted into a housing and attached to the front end RD20 preamplifier board and enclosure.

The PXS-II electronics, with its excellent imaging performance, is too bulky and high power for space based imaging (~25 Watts for a 20mm anode readout). NASA's Strategic Astrophysics Technology (SAT) program has funded the development of two application specific integrated circuits (ASICs) called the CSAv3 and the HalfGRAPH that would decrease the mass and power of the readout electronics while improving its event throughput performance by speeding up the preamps. [17]. A 16 channel (CSAv3) ASIC is a charge sensitive preamp that has a 20 ns risetime and returns to baseline in less than 100 ns. The 16 channel HalfGRAPH ASIC samples the preamp waveform at 1 GHz

and digitizes these analog samples with low power Wilkinson ADCs triggered by the preamp. Both these ASICs have been fabricated and tested and are currently being integrated together into an evaluation prototype.

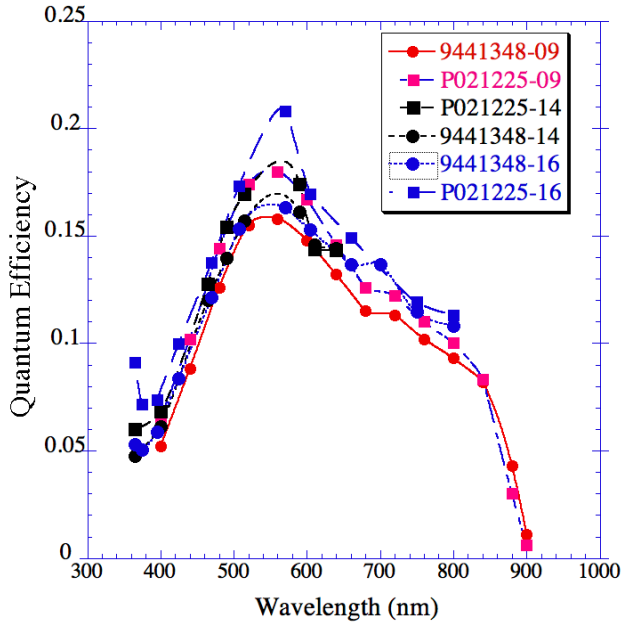


Fig. 7. Photocathode quantum efficiency for two 18 mm sealed tube cross strip anode detectors (Super-GenII cathodes) measured in 2009 and again in 2014 and 2016.

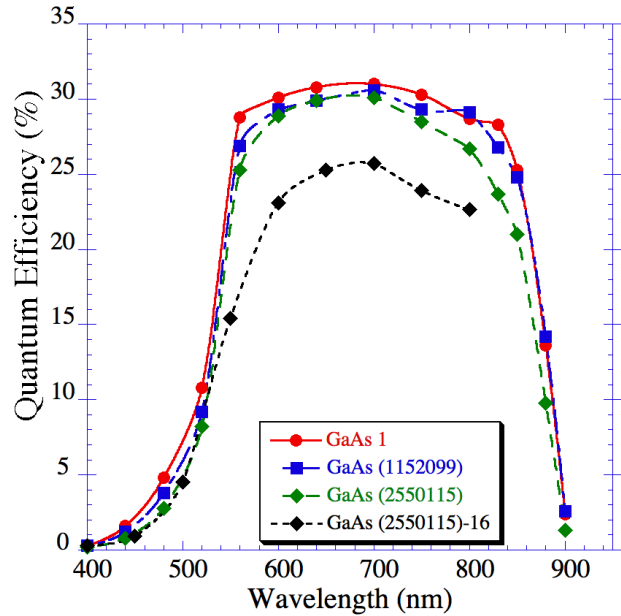


Fig. 8. Photocathode quantum efficiency for three 18 mm sealed tube cross strip anode detectors (GaAs photocathode) measured in 2012 and again in 2016.

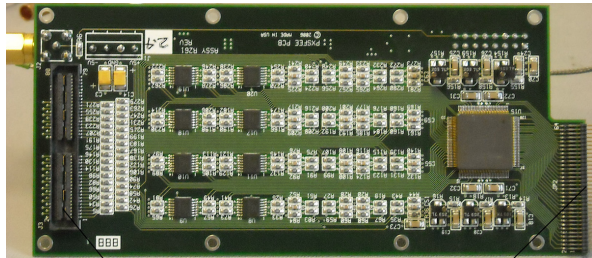


Fig. 9. 64 channel preamplifier board based on the 32 channel RD20 amplifier chip (right) ASIC. After post amplification the 40ns peaking time signals are sent to The main ADC board via shielded ribbon cables.



Fig. 10. PXS-II electronics. View shows two 32 channel 50 MHz ADC boards which digitize the amplifier signals. Below is a main board with a Xilinx Virtex-6 FPGA ASIC that calculates XY positions and provides a time stamp.

2.4 Cross Strip Sealed Tube Detector System Imaging Tests

The 18 mm photocathode area, 22 mm XS, sealed tube sensors were combined with the RD20 and PXS-II electronics, (Figs. 9, 10) to accomplish assessment of the spatial resolution and image linearity, gain uniformity and flat field characteristics. The overall image response uniformity in the 22 mm XS sealed tubes is often characterized by a residual fixed pattern noise banding that is stable, and usually less than ~7%, in both axes (Fig. 11). Banding occurs due to centroid calculation errors in the algorithm that estimates charge sharing between individual strips, and also depends on the gain, offset, crosstalk and noise variations of individual amplifiers. Further optimizations of the centroid algorithms to accommodate these issues reduces the effect. Finally, standard flat field data sets taken and divided out to correct the non-uniformities. An image representing average gain, instead of brightness, for the same flat field data of a

XS sealed tube (Fig. 12) offers information on the gain uniformity of the MCPs. The overall gain variation is less than 15%, but on a smaller scale the hexagonal pattern due to MCP multifibers is visible with a faint modulation (~5%).

Spatial resolution and image linearity evaluations are usually accomplished by imaging an array of small spots projected onto the photocathode surface. The spots are generally of the order 10 μ m wide with 1mm intervals (Fig. 13). The resolution is gain dependent but generally reaches a minimum at gains above 1×10^6 [10, 11]. Typical values are ~40 μ m (FWHM) for GaAs tubes and ~30 μ m (FWHM) for the Super-GenII tubes. The image distortion is low, with position errors less than 20 μ m over most of the field of view [17]. Also, the position resolution does not vary much over the field of view (Fig. 14).

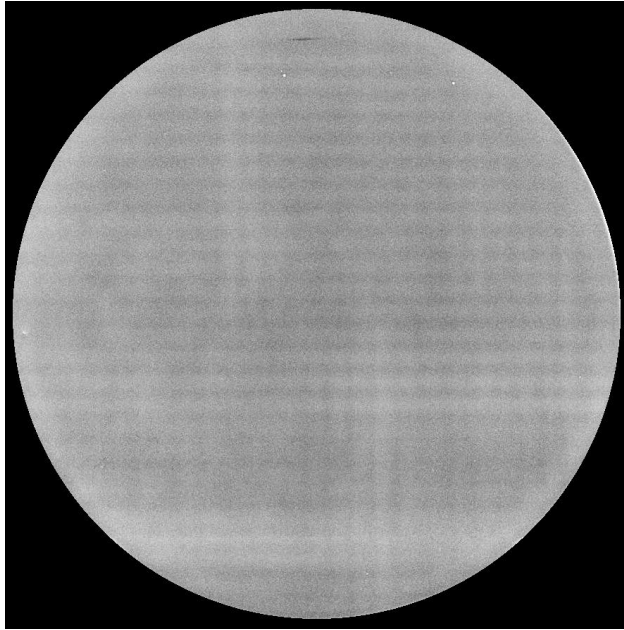


Fig. 11. 22 mm cross strip sealed tube with a Super-GenII cathode. Uniformly illuminated image has some anode modulation effect at the ~5 to 8% level. 1×10^6 gain.

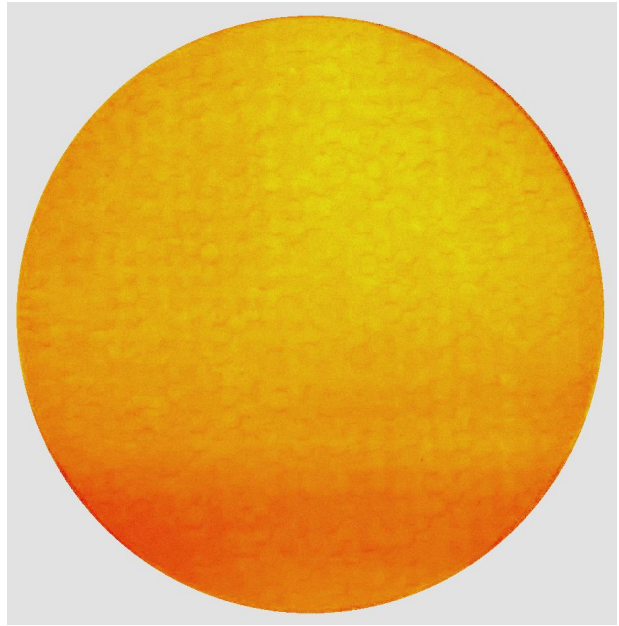


Fig. 12. 22 mm cross strip sealed tube with a Super-GenII cathode. Gain map image has less than 15% variations, and also shows a faint (5%) hexagonal MCP modulation.

2.5 Cross Strip Detector Event Rate and Time Tagging Performance

The overall event throughput of the cross strip readout MCP detector system is largely determined by the event processing electronics system. In the case of the PXS-II and RD20 amplifier system two main issues control the bandwidth. One is the recovery time of the amplifier and the other is the processing time of the ADC/FPGA system. The amplifier has a decay time of around 400 ns but this alone does not limit the rate as long as sequential events do not occur in the same position. The effective deadtime (non-paralyzable) of the PXS-II electronics is about 80 ns as determined by rate tests (Fig. 15), with ~ 82% event throughput at an input rate of 5 MHz. The local spot rate capability is determined by the detector not the electronics. The MCP detector is limited by the ability of the MCP pores to recharge between events which is a function of the MCP resistance, the area illuminated and the total charge gain of the MCP stack. For these sealed tubes measurements [11] have established rates of up to ~40 kHz in small areas (100 μ m) with an MCP stack having 60 M Ω resistance.

The high time resolution of MCP detector systems has enabled their use for a variety of timing applications including high time resolution astronomy [11], biological fluorescence imaging [8, 9], and LIDAR [7]. The 50 MHz sampling frequency of the PXS-II electronics can record a course time stamp of ~20 ns [14], which is sufficient for the majority of astronomical applications. For more demanding applications the timing resolution needed is closer to 100ps. This can be established using the signal at the output face of the MCP coupled to an additional timing channel. To accomplish this we use a high bandwidth preamplifier (Ortec VT120) attached to the bottom of the MCP stack. These ~2 ns wide signals are sensed with a constant fraction input discriminator having ~25 ps (FWHM) timing jitter and timed relative to an input trigger provided by the laser illumination, using a time to digital converter (3.7 ps bins).

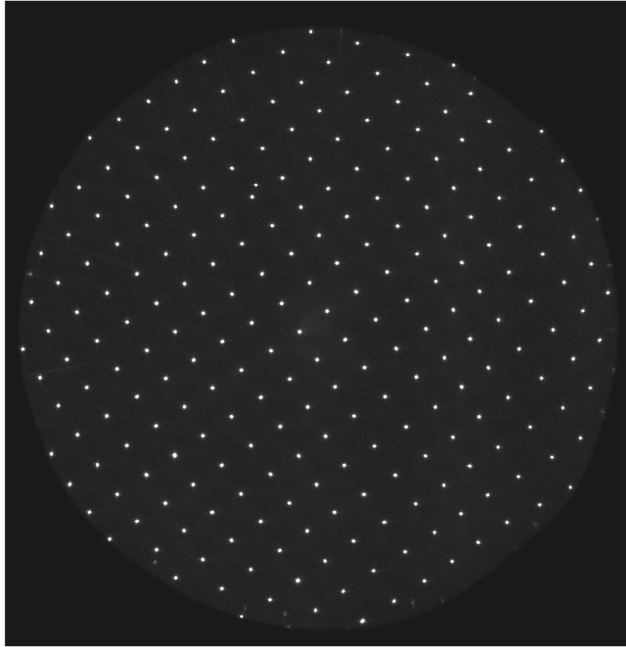


Fig. 13. Image of a projected pattern of 12 μm spots on 1 mm intervals using an 18 mm Super-GenII photocathode cross strip sensor with 120 V cathode-MCP gap bias.

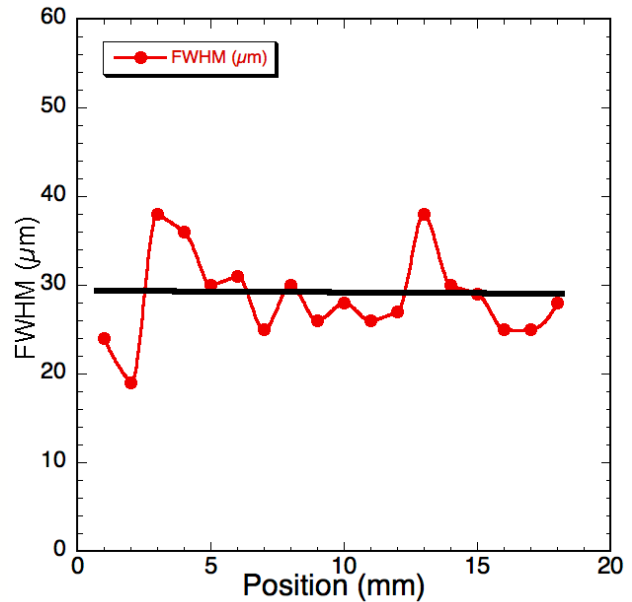


Fig. 14. Spatial resolution as a function of position for an 18 mm Super-GenII cathode (120 V bias) cross strip sensor with gain $\sim 2 \times 10^6$, average $\sim 29 \mu\text{m}$ FWHM.

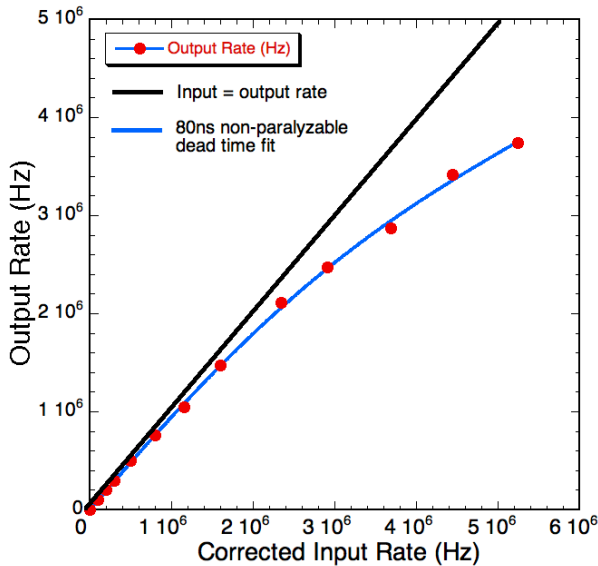


Fig. 15. Event rate processing capability for the PXS-II electronics with an 18 mm cross strip sensor system. Overall dead time is estimated at 80 ns per event.

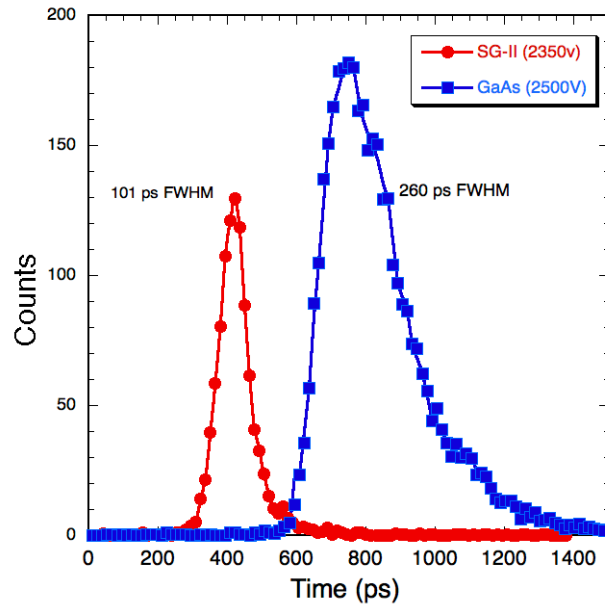


Fig. 16. Event timing error distributions for 18 mm Super-GenII and GaAs cross strip sensor systems at $\sim 2 \times 10^6$ gain. Spot illumination, 80 ps, 610 nm laser, 120 V cathode gap.

The time response distributions of the GaAs and Super-GenII cross strip sealed tubes were measured with a 610 nm pulsed laser (80 ps pulse width) having illumination spots $\sim 400 \mu\text{m}$ wide. The illumination was adjusted to produce only one photoelectron per laser pulse to evaluate the single photon detection regime. The Super-GenII results (Fig. 16) are ~ 100 ps FWHM at optimal settings, and the GaAs sealed tube timing resolution is ~ 260 ps FWHM. The poorer result for the GaAs photocathode is primarily due to the event transit time spread in the thick GaAs photocathode layer. Using a faster laser (Pilas, 630 nm, 45 ps) the result for the Super-GenII sealed tube photocathode does not change significantly. However, if the laser signal is increased up to ~ 100 photoelectrons per laser pulse, the timing distribution

narrows to about 55 ps FWHM. So with the better statistical error for large pulses the timing resolution becomes more consistent with the laser pulse width of 45 ps.

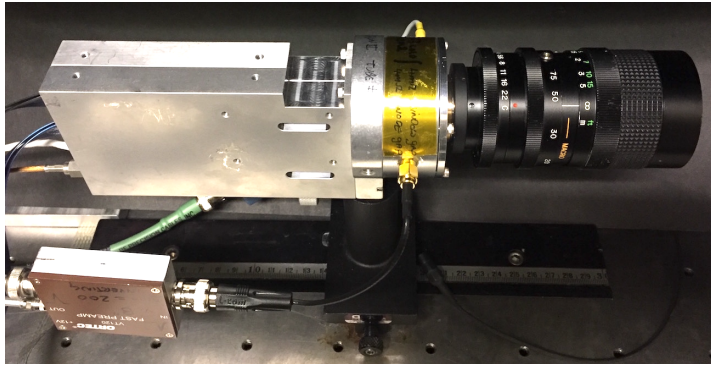


Fig. 17. Cross strip anode sealed tube sensor (Figs. 4, 6), with a Super-Gen II photocathode coupled to a macro lens system for imaging laser pulse reflections.



Fig. 18. Photograph of the teapot test object, which is roughly 15 cm diameter and 12 cm high.

Utilizing the high time resolution of this scheme we have performed a demonstration of 3D imaging with a 18 mm Super-Gen II photocathode cross strip tube with the PXS-II electronics and TDC. A standard camera lens was used to image events onto the detector (Fig. 17) and a Pylas 630 nm pulsed laser (45 ps) with a defocused beam (~25 cm diameter at the target) for illumination. A simple target with 3D structure was used, in this case a teapot (Fig. 18). The 2D image obtained with a photon counting rate at ~200 kHz (~1 detected photon per laser pulse) shows the target as illuminated by the laser is in accord with the object shape. The data was also recorded with the time interval between the laser trigger and the photon detection time as well as the X-Y position for each photon. The color coded image, representing time, in Fig. 20 provides a measure of the object depth profile. Closer portions are coded red and farthest away coded blue. A histogram cut through this image across the spout and body of the teapot shows that depth variations of considerably less than 1 cm are visible and are representative of the expected dimensions of the object.

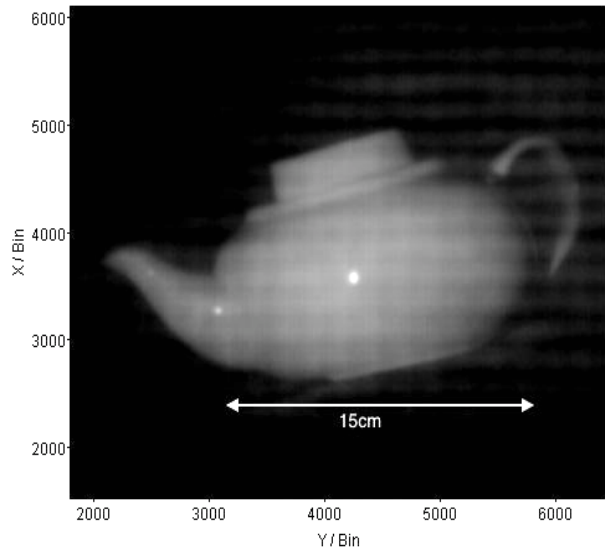


Fig. 19. Image of the teapot test object with the cross-strip sensor system. Illumination with a Pylas 630 nm pulsed laser (45ps wide). Only single photon events within the laser reflection time window are imaged.

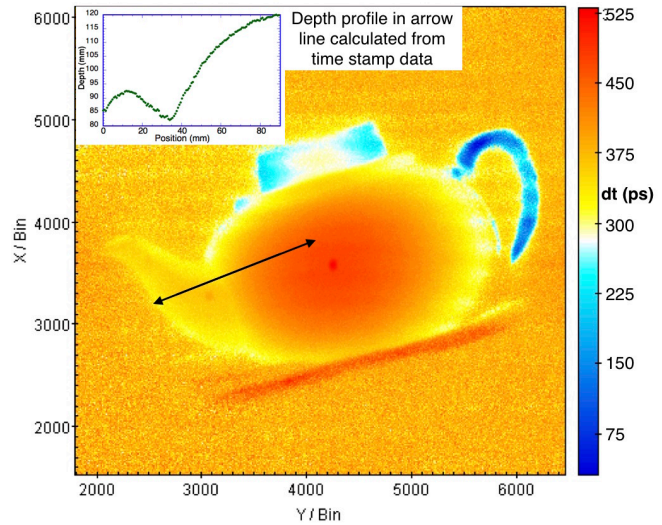


Fig. 20. Image of the teapot test object with the cross-strip sensor system with photon arrival time color mapping. Image depth variations of the <1 cm are clearly visible, which is in accord with system time sensitivity of <50 ps.

3. DEVELOPMENT PLANACON TUBES WITH ATOMIC LAYER MICROCHANNEL PLATES

Cross strip microchannel plate devices with formats up to 100 mm have been developed [18]. However, most imaging sealed tube devices have active areas less than about 5 cm and use conventional microchannel plates coupled to coarse pad array readouts [9]. The size limitations are partially due to limits on tube construction and on the

limitations of standard MCPs. Recently MCPs using borosilicate glass microcapillary arrays coated with atomic layer deposited resistive and secondary emissive layers [13, 18] have been made. These are attractive for sealed tube devices as they have low gas evolution and long lifetimes ($>7 \text{ C cm}^{-2}$) [13, 19] with physical robustness that permits large formats (400 cm^2), while enabling larger open areas ($>75\%$) that increase the photoelectron detection efficiency. Sealed tube compatible cross strip anodes have been made in formats up to $\sim 50 \text{ mm}$ [16] and could be used to make larger devices than the 18 mm field of view sealed tubes discussed in this paper.

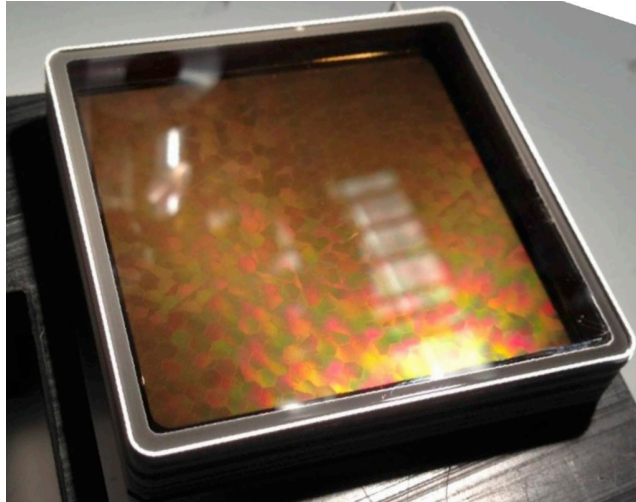


Fig. 21. Planacon sealed tube with a pair of $10 \mu\text{m}$ pore ALD borosilicate 60:1 MCPs and bi-alkali photocathode. 32×32 pad anode, with 2×2 pads joined for 8×8 format.

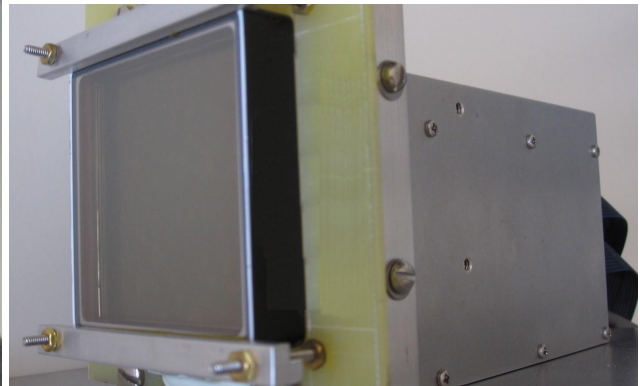


Fig. 22. Planacon sealed tube with 8×8 configuration (Fig. 21) anode coupled to a 64 channel RD-20 amplifier board for 2D imaging & timing with PXS-II electronics.

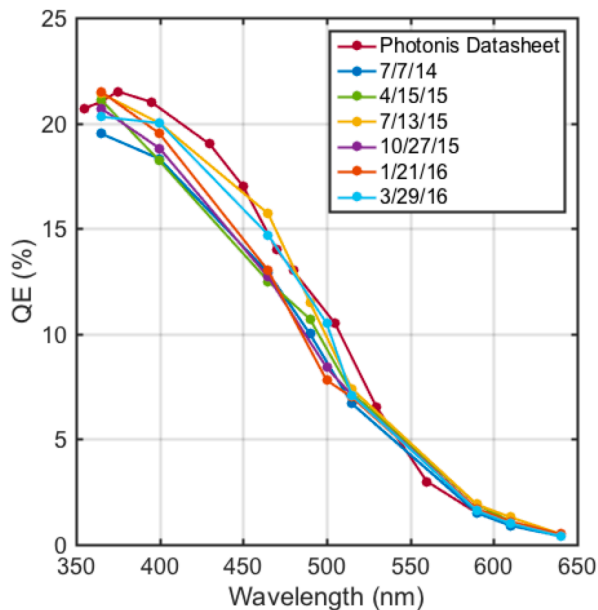


Fig. 23: Bi-alkali cathode quantum efficiency over time. 50 mm Planacon with a pair of 53 mm , $10 \mu\text{m}$ pore, 60:1 L/d, Al_2O_3 ALD borosilicate substrate MCPs.

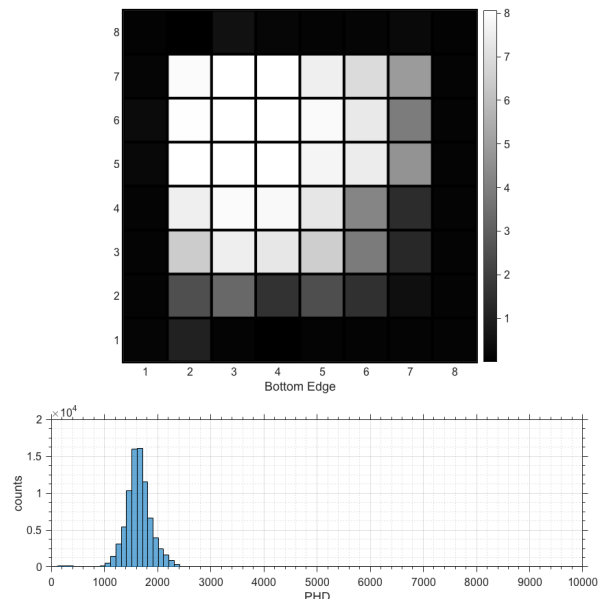


Fig. 24: Image of broad beam laser pulses over the upper left of the Planacon (Fig. 22). 80 ps , 610 nm laser, with ~ 10 photoelectrons/pulse, showing the event PHD below.

The Photonis Planacon provides a convenient commercial format with a $\sim 50 \text{ mm}$ active area (Fig. 21) to test the implementation of ALD MCPs in a sealed tube. In addition it can be configured for a variety of readout schemes. We have obtained a Planacon with a 32×32 anode pad array, which was supplied with a pair of $10 \mu\text{m}$ pore ALD MCPs each having 60:1 l/d and 8° pore bias. The photocathode was a standard bi-alkali and has a relatively large proximity gap ($\sim 5 \text{ mm}$). To test the tube and provide imaging capability the 32×32 pad anode was externally couple to a board which co-joined 2×2 pad areas to provide an 8×8 pad device. The 64 pads were then routed to the RD-20 amplifier

board (64 channels) (Fig. 22) and firmware was configured in the PXS-II electronics to count events in individual pad/pixels. The initial photocathode efficiency (Fig. 23) was in accord with expectations for standard Planacons. Repeated measurements over more than 2 years has shown that the efficiency has not measurably changed. The uniformity of the cathode was also good ($\pm 15\%$) with the lowest values at the corners of the active area [14].

In the current tests we used a defocused 610 nm laser to investigate the pulse response of the detector. Fig. 24 shows the relative rates for detection of individual laser pulses each producing the equivalent of ~ 10 photoelectrons from the photocathode. The laser was pointed roughly towards the upper left corner of Fig. 24 and was defocused to over a ~ 5 cm spot. The single photoelectron noise is equivalent to a gain of $\sim 1 \times 10^5$ with ~ 1000 V on each MCP and falls below the threshold for imaging and pulse detection. The pulse amplitude distribution is commensurate with our previous results and shows a narrow peak (Fig. 24). Individual events can be time tagged to ~ 20 ns with the PXS-II electronics, and if better time resolution is needed the MCP output signal can be utilized in the same fashion as the 18 mm devices to obtain sub ns timing. Prior results with Planacons [20] show single photon timing of ~ 70 ps FWHM. Future implementation of the Plancon with imaging/timing readouts, ALD MCPs and narrow gap proximity focus photocathodes potentially offer a larger format with long lifetime for 3D imaging applicable to a wide range of applications.

4. ACKNOWLEDGEMENTS

We wish to thank J. Hull, C. Scholz, J. McPhate, R. Raffanti, A. Martin, B. Welsh, J. Tedesco and the teams at Photonis and Incom, for their contributions to this work. This work was supported by NSF grants 0352980 and DBI-0552-096, NASA grants NNG11AD54G, NNX14AD34G, NNX12AF46A and NNX16AE92G.

5. REFERENCES

1. Siegmund, O.H.W., M.A. Gummin, J.M. Stock, et. al, Performance of the double delay line microchannel plate detect detectors for the Far-Ultraviolet-Spectroscopic Explorer, *Proc SPIE* 3114, pp.283-94 (1997).
2. Siegmund, O.H.W., P. Jelinsky, S. Jelinsky, et al., High resolution cross delay line detectors for the GALEX mission, *Proc. SPIE* 3765, pp.429-40 (1999).
3. Stock, J.M. O.H.W. Siegmund, J.S. Hull, et al., Cross-delay-line microchannel plate detectors for the Spectrographic Imager on the IMAGE satellite, *Proc SPIE* 3445, pp.407-14 (1998).
4. Siegmund, O.H.W., M.A. Gummin, T. Sasseen, et al., Microchannel plates for the UVCS and SUMER instruments on the SOHO satellite, *Proc. SPIE* 2518, pp.334-55 (1995).
5. Vallergera, J.; Zaninovich, J.; Welsh, B.; Siegmund, O.; McPhate, J.; Hull, J.; Gaines, G.; Buzasi, D. The FUV detector for the cosmic origins spectrograph on the Hubble Space Telescope, *Nuclear Instruments and Methods in Physics Research Section A*, Volume 477, Issue 1-3, p. 551-555 (2002).
6. Siegmund, O.H.W., J. McPhate, A. Tremsin, J.V. Vallergera, B.Y. Welsh and J.M. Wheatley, *AIP Conference Proceedings*, 984, 103 (2008).
7. Priedhorsky, W. and J. Bloch, *Applied Optics*, 44(3), 423-433 (2004).
8. Siegmund, O.H.W., J. Vallergera, P. Jelinsky, M. Redfern, X. Michalet, S. Weiss, "Cross Delay Line Detectors for High Time Resolution Astronomical Polarimetry and Biological Fluorescence Imaging", *IEEE Nuclear Science Symposium and Medical Imaging Conference*, (2005).
9. Michalet, X.; Siegmund, O. H. W.; Vallergera, J. V.; Jelinsky, P.; Millaud, J. E.; Weiss, S., Photon-counting H33D detector for biological fluorescence imaging, *Nuclear Instruments and Methods, A*, Vol. 567(1), p. 133 (2006).
10. Siegmund, O., J.V. Vallergera, A.S. Tremsin, J. McPhate, X. Michalet, S. Weiss, H.J. Frisch, R.G. Wagner, A. Mane, J. Elam, G. Varner. "Large Area and High Efficiency Photon Counting Imaging Detectors with High Time and Spatial Resolution for Night Time Sensing and Astronomy", *Advanced Maui Optical and Space Surveillance Technologies Conference*, (2012).
11. Siegmund, O.H.W. J.V. Vallergera, A. Tremsin, J. McPhate, B. Welsh "Optical Photon Counting Imaging Detectors with Nanosecond Time Resolution for Astronomy and Night Time Sensing" *Advanced Maui Optical and Space Surveillance Technologies Conference Proceedings*, p. E77 (2011).
12. Siegmund, O.H.W., J.B. McPhate, S.R. Jelinsky, J.V. Vallergera, A.S. Tremsin, R. Hemphill, H.J. Frisch, R.G. Wagner, J. Elam, A. Mane, "Large Area Microchannel Plate Imaging Event Counting Detectors With Sub-Nanosecond Timing," *IEEE Transactions on Nuclear Science*, 60(2), pp. 923-931 (2013).
13. Siegmund, O., N. Richner G. Gunjala, J.B. McPhate, A.S. Tremsin, H.J. Frisch, J. Elam, A. Mane, R. Wagner, C.A. Craven, M.J. Minot, *Proc. SPIE* 8859, 88590Y (2013).

14. Siegmund, O.H.W; Vallerger, J.; Tremsin, A.; Hull, J.; Elam, J.; Mane, A., “Optical and UV Sensing Sealed Tube Microchannel Plate Imaging Detectors with High Time Resolution”, Proceedings of the Advanced Maui Optical and Space Surveillance Technologies Conference, E10, 2014.
15. Adriani, O. *et al* "Beam test results for single- and double-sided silicon detector prototypes of the CMS central detector, “Nuclear Instruments and Methods in Physics Research A, 396, pp.76-92, (1997)
16. Siegmund, O.H.W., J. V. Vallerger, A. S. Tremsin, J. McPhate, X. Michalet, R. A. Colyer, S. Weiss, Microchannel Plate Imaging Photon Counters for Ultraviolet through NIR Detection with High Time Resolution, *Proc. SPIE* 8033, pp. 80330V-80330V-12 (2011).
17. Vallerger, J.V. J. McPhate, A. Tremsin, O. Siegmund, R. Raffanti, H. Cumming, A. Seljak, V. Virta and G. Varner, Development of a flight qualified 100 x 100 mm MCP UV detector using advanced cross strip anodes and associated ASIC electronics, *Proc. SPIE*. 9905-161, 2016.
18. Siegmund, O., J. McPhate, A.S. Tremsin, J.V. Vallerger, H.J. Frisch, R.G. Wagner, A. Mane, J. Elam, G. Varner. “Large Area flat panel Photon Counting Imaging Detectors for Astronomy and Night Time Sensing”, Advanced Maui Optical and Space Surveillance Technologies Conference, (2013).
19. Lehmann, A. *et al*. Improved lifetime of microchannel-plate PMTs *Nuclear Instruments and Methods in Physics Research A* 766 (2014) 138–144.
20. Va’vra, J., C. Ertley, D.W.G.S. Leith, B. Ratcliff, J. Schwiening, A high-resolution TOF detector—A possible way to compete with a RICH detector *Nuclear Instruments and Methods in Physics Research A* 595 (2008) 270–273.